Laboratory and numerical investigation of direct shear box test

Dániel Horváth*, Tibor Poós† and Kornél Tamás+

*†Department of Building Services and Process Engineering
Budapest University of Technology and Economics (BME), Faculty of Mechanical Engineering
Bertalan Lajos street 4-6. Building D110, H-1111 Budapest, Hungary
*e-mail: horvath.daniel@mail.bme.hu, † e-mail: poos@mail.bme.hu
web page: https://www.epget.bme.hu/en/

+Department of Machine and Product Design
Budapest University of Technology and Economics (BME), Faculty of Mechanical Engineering
Bertalan Lajos street 4-6. Building MG300, H-1111 Budapest, Hungary
e-mail: tamas.kornel@gt3.bme.hu, web page: http://www.gt3.bme.hu/en/

ABSTRACT

In agriculture, food, chemical, plastic and pharmaceutical industries for designing and operating machines, it is essential to determine the mechanical parameters of the processed granular materials. In most cases, these characteristics are the internal friction angle, the contact cohesion developed by the surface moisture and the apparent cohesion occurred by the shape of the granular material. Further physical quantities are required to characterize the motion state of the particles, which were determined by laboratory measurements in this study. Hulled millet was used for the measurements because its geometric shape can be modeled as sphere in the numerical investigations with good approximation. The porosity, the particle and bulk density of the hulled millet were determined by means of an air pycnometer in case of several moisture content. Using laboratory direct shear box test, under standard conditions, the shear strength of the cohesive liquid bridges and the internal friction angle in the bulk were determined. The results obtained were used for input parameters of a discrete element model. The aim of this research was to determine the micromechanical parameters by simulation, based on the macromechanical results of the hulled millet bulk during laboratory measurements.

1. INTRODUCTION

In the industry, it is necessary to know the physical and mechanical properties of the processed materials in order to operate and design different machines. Such parameters can be, for example, the angle of repose and the internal friction angle of the materials in agriculture and food industry, as well as their bulk and particle density. It is important to distinguish between dry and wet material bulks, as the moisture content of the surface and the material can greatly affect the movement and behavior of the bulk. Nowadays, various design and operation tasks are supported by computerized numerical models. Discrete Element Method (DEM) is a solution for modeling the movement of granular materials, which builds up a particle assembly from discrete elements with their own micromechanical parameters during the simulations [1]. Thus, we can distinguish between the mechanical parameters of the macro- and micromechanical, ie. the bulk-level and the one-particle only. The former is used for operational planning and operation, and the latter for computer modeling and other grain processing operations (eg. hulling, seed separation, cleaning, grinding, etc.).
C. J. Coetzee (2016) [2] described the steps of a DEM model calibration procedure and the effects of the particle shape. In his research, he determined some macromechanical material properties of crushed stones of less than 40 mm size by laboratory measurements and calibrated each micromechanical material parameters with DEM simulations. The internal friction angle was determined between particle-particle with direct shear box tests and angle of repose tests. He pointed out that the internal friction angle values obtained by the angle of repose tests

should be handled with care because they may prove to be low in other applications. In the DEM simulations, a particle model of linear springs, viscous dampings and Coulomb friction was used to model the real processes.
In the research of Tamás K. *et al.* (2015) [3], mechanical properties of rapeseed were determined by measurements and DEM simulations, in which a particle contact model consisting of liner springs, viscous dampings and Coulomb friction was also used to describe the collisions between the particles. In addition, the adhesion forces created by the surface moisture between the particles were modeled by cohesive bonds. In their research, direct shear box test was used, but the effect of the moisture content was not investigated.
J. Horabik and M. Molenda (2016) [4] collected micromechanical parameters of agricultural crops and different DEM contact models used in the studies of other researchers. Considering the absorbent effects of each material, ranges were given for each material properties, but based on the parameters collected in this way, it is not possible to determine the range and function characteristics of the domains depending on the moisture content.
In this study, DEM numerical simulations were carried out using cohesive-frictional contact model [5]. After developing the model of the direct shear box test and using the macromechanical parameters obtained from the laboratory measurements, micromechanical parameters were determined. These were the rolling and twisting resistance coefficients and the normal and shear strengths of the cohesive bonds depending on the moisture content of the material. The aim of this research was to determine the micromechanical parameters by simulations, based on the macromechanical results of the hulled millet bulk during laboratory measurements.

2. MATERIAL AND METHOD

2.1. Material

In this research, hulled millet (Panicum miliaceum L.) was used, which is illustrated in Fig. 1.

Figure 1. Hulled millet (Panicum miliaceum L.)

Before the measurements, the impurities and the broken particles were removed by the wind classification device, and the nearly homogeneous distribution of particles was created in the examined bulk. The material was wetted in a uniquely made rotating drum unit, into which a certain amount of millet and water was loaded. The drum was operated for 4 hours and it mixed the material at 10 minutes intervals for 2 minutes. The method for determining the moisture content of the hulled millet is to dry a sample from the bulk to constant weight at 105±5 °C which takes generally about 24–48 h. By weighing the wet sample before drying

(m_{wm}) and after drying (m_{dm}), the moisture content on wet basis of the material could be calculated:

$$x = \frac{m_{wm} - m_{dm}}{m_{wm}} \cdot 100\% \quad (1)$$

The typical diameter of the hulled millet was $d = 1.8\,mm$, which was determined by sieve analysis and the moisture content-dependent particle density by air pycnometer [6].

2.2. Experimental method

Using direct shear box tests, geotechnical investigations can be carried out primarily, but nowadays, with the widespread use of discrete element modeling, researchers are also using it for investigating larger granular materials [2], [3], [7], [8]. The operation of the equipment is based on the shearing of the particulate material bulk and the measurement of the resulting shear force at different normal direction loads which produces the normal stresses. The standard rectangular device used in laboratory measurements is illustrated in Fig. 2.

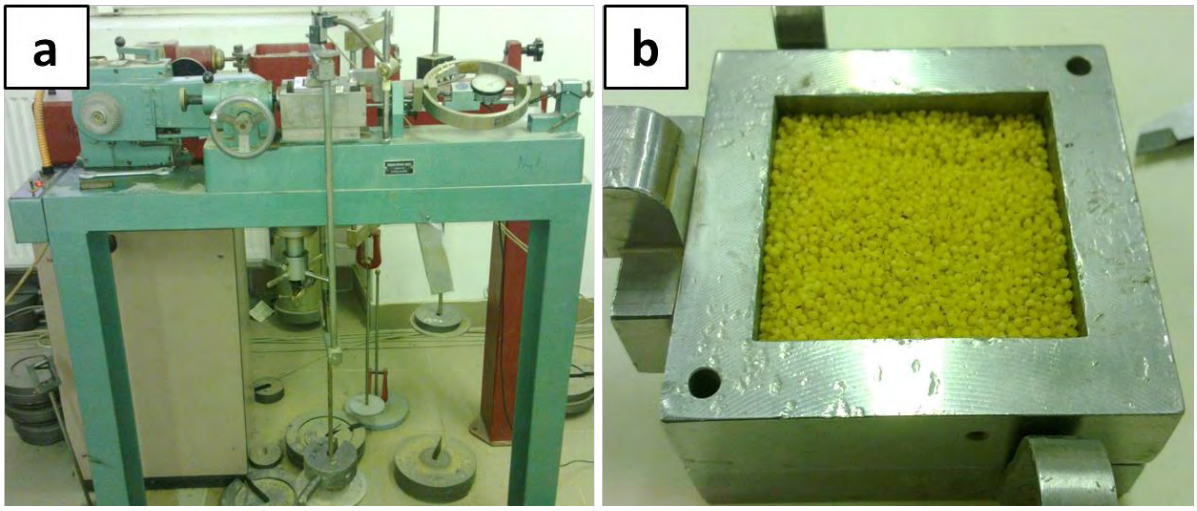

Figure 2. The laboratory direct shear box (a), and the shear box filled with hulled millet (b)

The standard laboratory direct shear box apparatus had an inner size of 60×60×30 mm where the granular material could be loaded. The shear speed of $v_{shear} = 0.02\,mm/s$ and shear displacement of $h = 6 - 9\,mm$ were set based on [9]. During the measurements, shear tests were carried out using $\sigma_{load} = 11.96; 19.61; 29.42\,kPa$ normal loads, and the evaluation was performed according to standard [8]. The shear force, shear displacement and time were recorded during the measurement. For a given normal load, by knowing the shear cross-section ($A = 60 \cdot 60 = 3600\,mm^2$) and the measured maximum shear force ($F_{shear,max}$), the maximum shear strength of the granular material could be determined:

$$\tau_{shear,max} = \frac{F_{shear,max}}{A} \quad (2)$$

By illustrating the maximum shear strength (τ_{max}) and the normal load (σ) point pairs and then fitting a linear trend line, the failure envelope of the granular assembly can be obtained. The slope of the failure envelope defines the internal friction angle (φ'), and the axis section to the macromechanical apparent and contact cohesion shear strength of the particle assembly ($\tau_{coh,ma}$).

2.3. Discrete element method

For numerical simulations, the Yade open-source discrete element software [10] was used, in which the model building can be done using *python* programming language. Cohesive-frictional particle contact model (CohFrictMat) illustrated in Fig. 3 was utilized to model the rheological processes between the particles, in which the tensile forces resulting from the interparticle liquid can be modeled with bonds [5].

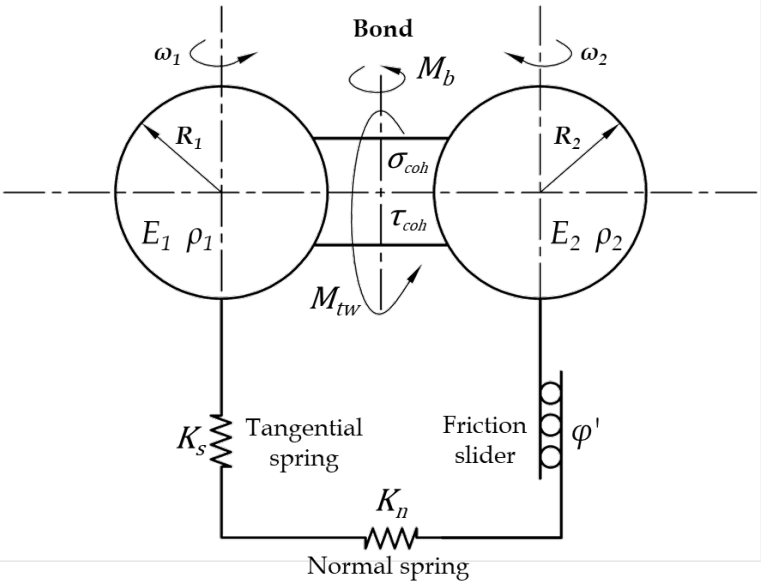

Figure 3. The schematics of the cohesive-frictional contact model (CohFrictMat)

The particle contact model consists of a normal and a tangential linear spring and a friction slider modeling the Coulomb friction. Cohesive bond can be modeled as a rigid beam behavioral element that can break due to tensile force in normal direction. In case of a particle collision, the normal contact stiffness (K_n) can be calculated from the modulus of elasticity of the colliding particles ($E_1; E_2$) and the radius of the particles ($R_1; R_2$), taking the harmonic average of the parameters:

$$K_n = 2\frac{E_1R_1E_2R_2}{E_1R_1+E_2R_2} = 2\frac{k_{n1}k_{n2}}{k_{n1}+k_{n2}} \tag{3}$$

The tangential contact stiffness (K_s) can be given by a proportional factor (υ), which can be used to control the Poisson ratio indirectly:

$$K_s = \upsilon K_n = 2\frac{E_1R_1\upsilon_1E_2R_2\upsilon_2}{E_1R_1\upsilon_1+E_2R_2\upsilon_2} = 2\frac{k_{s1}k_{s2}}{k_{s1}+k_{s2}} \tag{4}$$

The normal force vector occurring during the collision of the particles can be calculated from the normal contact stiffness, the normal overlap of the particles (u_n) and the normal vector ($\underline{n}$) perpendicular to the collision plane:

$$\underline{F_n} = K_n u_n \underline{n} \tag{5}$$

The resulting shear force vector can be calculated from the tangential contact stiffness, the tangential velocity ($\underline{v_s}$), and the time step (Δt) using incremental formulation that takes into account the value of one time step earlier:

$$\underline{F_s}^t = \underline{F_s}^{t-\Delta t} + K_s \underline{v_s} \Delta t \tag{6}$$

The maximum shear force can be determined from the normal force, the internal friction angle (φ') and the shear strength of the cohesive bond ($F_{coh,s}$) which is zero if there is no cohesive bond between the colliding particles:

$$F_{s,max} = \left|\underline{F_n}\right| tan(\varphi') + F_{coh,s} \tag{7}$$

If the arising shear force during the collision exceeds the maximum allowed for elasticity, ie. $\left|\underline{F_s}\right| > F_{s,max}$, the shear force must be limited to meet the elasticity conditions and to slip:

$$\underline{F_s}^{limited} = \underline{F_s} \frac{F_{s,max}}{|\underline{F_s}|} \tag{8}$$

Based on these, the force vector arising in the contact point during the collision is:

$$\underline{F} = \underline{F_n} + \underline{F_s} \tag{9}$$

The normal ($F_{coh,n}$) and shear force ($F_{coh,s}$) of the cohesive bonds can be calculated from the normal (σ_{coh}) and the shear strength (τ_{coh}) using the radiuses of the particles in contact:

$$F_{coh,n} = \min\left(\sigma_{coh,1}; \sigma_{coh,2}\right) \min(R_1; R_2)^2 \tag{10}$$

$$F_{coh,s} = \min\left(\tau_{coh,1}; \tau_{coh,2}\right) \min(R_1; R_2)^2 \tag{11}$$

If the arising normal force exceeds the normal-direction cohesive force, ie. $\left|\underline{F_n}\right| > F_{coh,n}$, the cohesive bond breaks between the two particles. There are two options for activating the cohesive bonds in the software. One is the '*setCohesionNow*' command [11], which is used to activate the cohesive bonds between the overlapping ($u_n > 0$) particles at the given time step, and not after the bond breaking at later time steps. The other command is '*setCohesionOnNewContacts*' [11], which, after activation, creates cohesive bond at any later time step in case of particle overlapping. In the presence of cohesion bonds, the particles cannot roll freely and cannot twist freely, and in reality the shape of the particles is not a perfect sphere. In this way, bending and twisting torques have been introduced to adjust the above-mentioned aspects. To determine the torques, first, the relative angular velocity vector is required, which can be calculated from the angular velocity vector ($\underline{\omega_1}; \underline{\omega_2}$) of the two colliding particles:

$$\underline{\omega_{rel}} = \underline{\omega_2} - \underline{\omega_1} \tag{12}$$

The rolling component of the relative angular velocity vector can be defined as follows:

$$\underline{\omega_{rel,b}} = \underline{\omega_{rel}} - \underline{\omega_{rel,tw}} \tag{13}$$

Twisting component of relative angular velocity vector:

$$\underline{\omega_{rel,tw}} = \left(\underline{\omega_{rel}} \cdot \underline{n}\right)\underline{n} \tag{14}$$

The rolling stiffness can be given by a proportionality factor (α_{kr}) relative to the radius of the particles and the tangential contact stiffness:

$$K_r = R_1 R_2 K_s \alpha_{kr} \tag{15}$$

It should be noted that recent literature [12] has shown that the rolling stiffness should be compared to normal contact stiffness instead of tangential contact stiffness. Similarly, the twisting stiffness can be calculated with another proportionality factor (α_{ktw}) as the rolling stiffness:

$$K_{tw} = R_1 R_2 K_s \alpha_{ktw} \tag{16}$$

Finally, the bending (M_b) and the twisting torque (M_{tw}) can be determined using an incremental formulation that takes into account the previous value of one time step:

$$\underline{M_b}^{t} = \underline{M_b}^{t-\Delta t} - K_r \underline{\omega_{rel,b}} \Delta t \tag{17}$$

$$\underline{M_{tw}}^{t} = \underline{M_{tw}}^{t-\Delta t} - K_{tw} \underline{\omega_{rel,tw}} \Delta t \tag{18}$$

The maximum allowable bending ($M_{b,max}$) and twisting torque ($M_{tw,max}$), which still satisfy the elasticity conditions, can be calculated using the rolling (η_r) and the twisting resistance coefficient (η_{tw}):

$$M_{b,max} = \left|\underline{F_n}\right| \min(\eta_r R_1; \eta_r R_2) \tag{19}$$

$$M_{tw,max} = \left|\underline{F_n}\right| \min(\eta_{tw} R_1; \eta_{tw} R_2) \tag{20}$$

Similarly to the determination of the rolling stiffness, it is advisable to determine the maximum twisting torque with shear force instead of the normal force, based on literature [12]. If the resulting bending torque exceeds the maximum value, it must be controlled to meet the elasticity conditions:

$$\underline{M_b}^{limited} = \underline{M_b} \frac{M_{b,max}}{|\underline{M_b}|} \tag{21}$$

Similar to bending torque, the twisting torque must also be limited:

$$\underline{M_{tw}}^{limited} = \underline{M_{tw}} \frac{M_{tw,max}}{|\underline{M_{tw}}|} \tag{22}$$

The critical time step calculated by the software is used to select the appropriate time step. The critical time step is given by the smallest value calculated from the particle radius, the particle density, and the modulus of elasticity, which calculation is done using all (i) particles [10], [13]:

$$\Delta t_{crit} = \min_i R_i \sqrt{\frac{\rho_{p,i}}{E_i}} \tag{23}$$

Since there is no speed-dependent damping in the presented contact model, numerical (artificial) damping (λ_d) can be used to dissipate the kinetic energy of the particles. This is done by reducing the $\underline{F_i}$ forces which increase the speed of the particles by ΔF_d force, taking into account the speed ($\underline{v_i}$) of the particles and their acceleration ($\underline{a_i}$) [9]:

$$\frac{\underline{\Delta F_d}}{\underline{F_i}} = -\lambda_d \mathrm{sgn}\underline{F_i} \left(\underline{v_i} + \frac{\underline{a_i} \Delta t}{2}\right) \tag{24}$$

Based on these, the damping mechanism is not a physical but an artificial quantity, because the damping is done with a component that is not invariant with respect to the coordinate system rotation. The resting state of the examined particle assembly can be measured with the unbalanced force ratio during the simulations. This parameter specifies the ratio of the average of all forces exerted on the bodies and the magnitude of the average force in the contacts. In case of perfect static equilibrium, the total exerted force on the bodies is zero, so the ratio tends to zero. Meanwhile, the discrete elements of the simulation are stabilized and thus come to resting state. However, the ratio never takes zero value because of the finite precision computation.

2.4. Discrete element model

The DEM model of the direct shear box test was built on 1:1 scale based on the laboratory equipment. The two part of the shear box and the load plate were modeled as structure walls. The lower box was open at the top and the upper box was open at the top and the bottom side. The material parameters of the structure walls were taken from the material properties of steel [4]. The steel had a density of 7750 kg/m^3, a modulus of elasticity of 200 GPa, a proportional parameter between normal and tangential contact stiffness of 0.3, and an internal friction angle of 40.1°. To fill the boxes with particles, gravity deposition was used, to which a bottom side open box was placed in our model over the upper shear box so that the particles did not fall out during the process. Due to the wall thickness of the boxes, square shapes were used in the shear direction to prevent the particles from falling out of the boxes during the simulations. In order to provide the normal load, an infinitely wide structure wall was used. It did not have a

mass, but at a given speed, it moved as a servo drive at the top of the particle set in the same or opposite direction as the gravity acceleration. This was necessary because, during the laboratory measurements, the load plate moved upwards too in the vertical direction as a result of shearing. The appropriate normal load was set by measuring the force exerted by the particles on the element modeling the load plate. The DEM model of the direct shear box and the simulation steps are illustrated in Fig. 4.

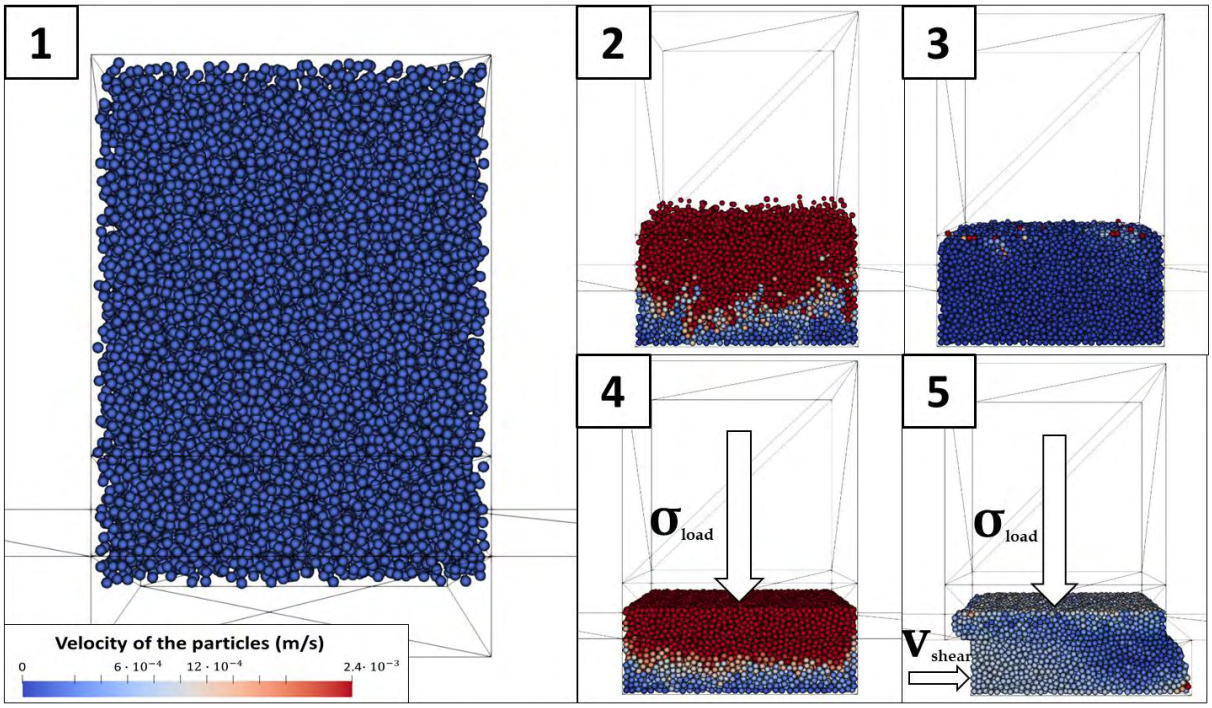

Figure 4. DEM model of the direct shear box test and the steps of the simulation (1. generating particles; 2. gravity deposition of the particles; 3. activating cohesive bonds; 4. application of load plate; 5. start of shearing)

The first step of the simulation was the generation of the particles (Fig. 4/1) followed by the gravity deposition (Fig. 4/2). After the stabilization of the particle set, when the unbalanced force ratio dropped below 0.001, the cohesive bonds were activated using the '*setCohesionNow*' command (Fig. 4/3). This was followed by the application of the normal load (σ_{load}) (Fig. 4/4), then at the speed of $v_{shear} = 1 \frac{mm}{s}$, the shearing was started by moving the lower shear box (Fig. 4/5). The increase in the shear velocity compared to the laboratory measurements ($v_{shear} = 0.02\ mm/s$) was used to reduce the computational time requirement. It was assumed that the increase in shear speed does not affect the maximum shear force value but only the position of it at the shear length [9]. The resulting shear force was measured on the right-hand side of the upper shear box illustrated in Fig. 4/1 at a sampling interval of 0.1 s. The hulled millet particles were modeled with spheres with a normal distribution of $d = 1.8 \pm 0.1\ mm$, The particle density (ρ_p) of the hulled millet was chosen based on preliminary air pycnometer measurements, the elasticity modulus ($E = 20\ MPa$) and the proportional parameter between normal and tangential contact stiffness ($\upsilon = 0.2$) were selected from the literature [4] and the internal friction angle (φ') was set based on previous simulation experience. The additional values of the setting parameters are summarized in Table 1.

Table 1. DEM material parameters of hulled millet

No.	Measured x [%]	Selected ρ_P [kg/m³]	Measured φ' [°]	Set Δt [s· 10^{-6}]
1	11.2	1379	42.2	4.7
2	16.1	1388	42.1	4.8
3	18.7	1393	41.6	4.8
4	23.6	1402	40.5	4.9
5	24.1	1403	38.7	4.9
6	28.2	1410	37.5	5

The time steps used in the simulations were set lower than the critical time step obtained by Eq. (23). The numerical damping value was $\lambda_d = 0.5$ and 21000 particles were modeled. The normal (σ_{coh}) and shear strengths (τ_{coh}) of the cohesive bonds were determined by simulation calibrations, as well as the rolling (η_r) and twisting resistance coefficients (η_{tw}), which are presented in the *Results* section.

3. RESULTS

Fig. 5 illustrates the measurement and simulation results of the direct shear box test where the shear force (F_{shear}) - shear displacement (h) results can be seen at different normal loads ($\sigma_{load} = 11.96\ kPa; 19.61\ kPa; 29.42\ kPa$) for $x = 18.7\%$ moisture content hulled millet.

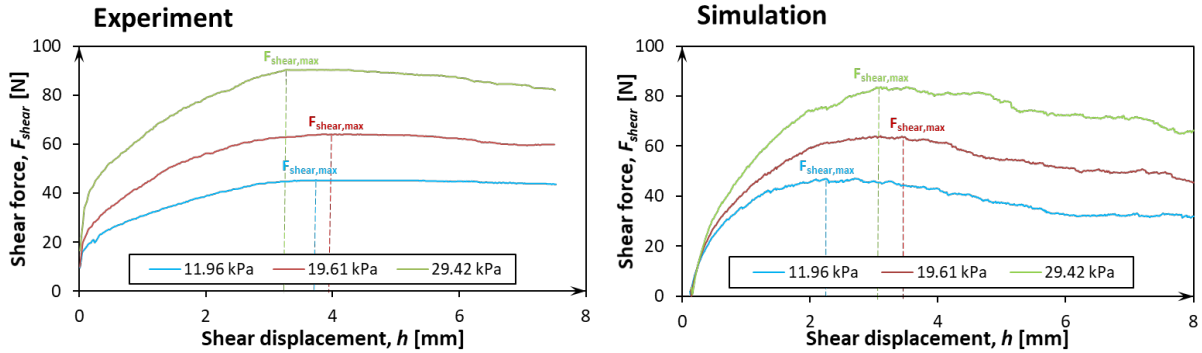

Figure 5. The measured (left side) and simulated (right side) shear force as a function of shear displacement at different normal loads for x=18.7% moisture content hulled millet

In the simulation results - compared to the measurements -, the steeper reductions in the forces seen after the maximum shear forces were due to the use of artificial damping and higher shear speed [9]. However, the results showed a good match as the maximum shear forces occurred at almost the same shear displacement for $\sigma_{load} = 19.61\ kPa; 29.42\ kPa$ normal loads. By calculating the shear stresses from the maximum shear forces, and illustrating them as a function of the associated normal loads, the failure envelopes shown in Fig. 6. could be plotted.

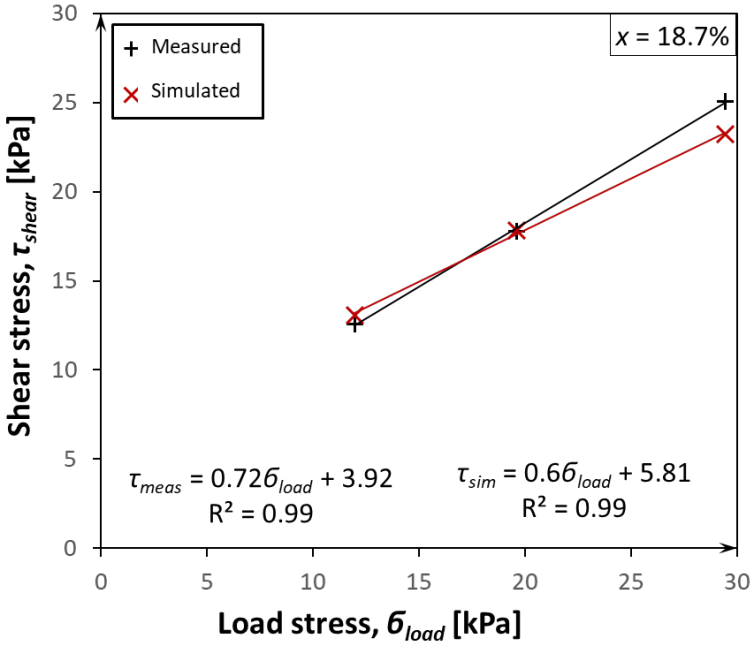

Figure 6. The failure envelopes in case of x=18.7% moisture content hulled millet, obtained by measurements and DEM szimulations

In the simulation calibrations, the unknown micromechanical cohesive normal and shear strengths were set equally for a specific moisture content based on own simulation experience. The values of the rolling and twisting resistance coefficients were also treated equally, but they gave a value of $\eta_r = \eta_{tw} = 0.05$ regardless of the moisture content. In the simulation results, the cohesive strengths could be used to change the axis section of the failure envelopes, but by changing the resistance coefficients, the slopes of the lines could be influenced. The calibrated micromechanical cohesive normal and shear strengths are plotted against the moisture content in Fig. 7.

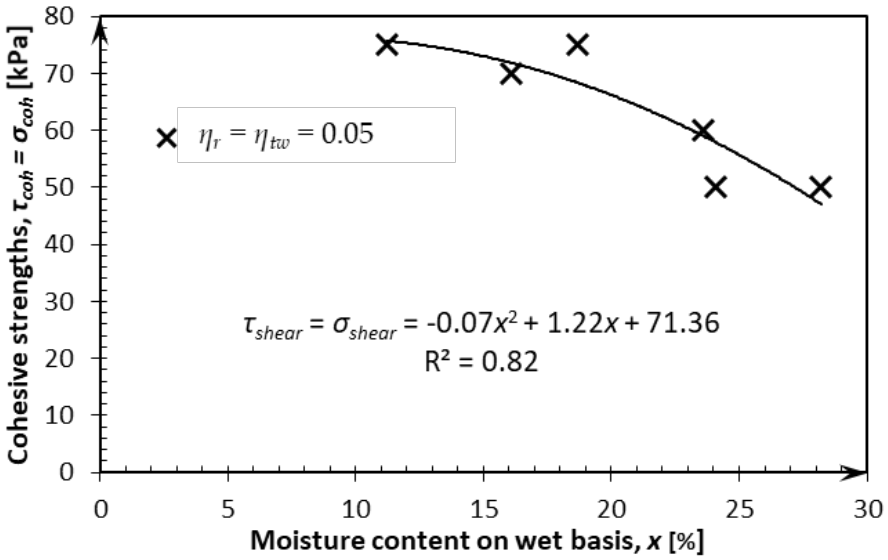

Figure 7. The micromechanical cohesive strengths of the bonds obtained by DEM simulations as a function of the moisture content of the hulled millet for $\eta_r = \eta_{tw} = 0.05$ resistance coefficents

The function fitted to the data showed a second order polynomial nature, which means that it is not enough to specify a domain for each micromechanical parameter, but also to define the function nature so that it can be used more accurately for later DEM simulations. The accuracy of the simulation results was characterized by the relative errors between the measured

($\tau_{shear,measured}$) and simulated shear strengths ($\tau_{shear,simulated}$), which were calculated as follows:

$$Relative\ error = \left|\frac{\tau_{shear,simulated} - \tau_{shear,measured}}{\tau_{shear,measured}}\right| 100\% \quad (25)$$

The measured and simulated maximum shear strengths for different moisture contents and normal loads, and the relative errors are summarized in Table 2.

Table 2. Measured and simulated maximum shear strengths, moisture contents, normal loads and the calculated relative errors

No.	x [%]	σ_{load} [kPa]	$\tau_{shear,measured}$ [kPa]	$\tau_{shear,simulated}$ [kPa]	Relative error [%]
1	11.2	11.96	14.42	13.86	3.9
2		19.61	17.42	17.92	2.9
3		29.42	25.47	23.53	7.6
4	16.1	11.96	14.42	13.22	8.3
5		19.61	18.61	18.69	0.4
6		29.42	24.86	25.14	1.1
7	18.7	11.96	12.58	13.06	3.8
8		19.61	17.78	17.83	0.3
9		29.42	25.06	23.22	7.3
10	23.6	11.96	11.97	12.28	2.6
11		19.61	17.11	17.08	0.2
12		29.42	24.11	23.11	4.1
13	24.1	11.96	10.19	11.28	10.6
14		19.61	16.25	16.14	0.7
15		29.42	22.89	21.81	4.7
16	28.2	11.96	10.31	10.19	1.1
17		19.61	15.19	15.06	0.9
18		29.42	21.97	20.61	6.2

The highest relative error (10.6%) between the measured and simulated results was at $x = 24.1\%$ moisture content and 11.96 kPa normal load. In other cases, the results of the laboratory measurements were modeled with relative error less than 10% using the previously defined DEM micromechanical parameters.

4. CONCLUSION

In this research, direct shear box tests were performed using hulled millet in case of different moisture contents. The discrete element model of the laboratory equipment was created, using a cohesive-frictional particle contact model to model the collisions of the particles and the cohesive forces resulting from the surface moisture of the material. The main goal was to determine the micromechanical parameters describing the cohesion relationships and their moisture-dependent behavior. These were the cohesive normal and shear strengths, and the rolling and twisting resistance coefficients that were less dependent of the moisture content. By varying the former two parameters equally, the axis section of the failure envelopes - obtained by the direct shear box simulations - could be changed, while the latter two variables could be used to influence the slopes. Based on these, it was possible to simulate the measurement results with just one parameter set combination in case of a moisture content. Cohesive strengths were determined at moisture content range of $11.2 - 28.2\%$. The points thus obtained were described by a second-degree polynomial function with good accuracy and can be used for future DEM simulations.

ACKNOWLEDGEMENT

This work was supported by Richter Gedeon Talentum Foundation (19-21. Gyömrői street, 1103 Budapest. Hungary) and the Higher Education Excellence Program of the Ministry of Human Capacities in the frame of Water science & Disaster Prevention and Artificial intelligence research area of Budapest University of Technology and Economics (BME FIKP-VÍZ, BME FIKP-MI). We also greatly appreciate the financial funding provided by 'Richter Gedeon Nyrt. Centenáriumi Alapítvány' (H-1103 Budapest, Gyömrői str. 19-21., Hungary) and 'Gépészmérnök-képzésért Alapítvány' (H-1111 Budapest, Műegyetem rkp. 3., Hungary).

REFERENCES

[1] Cundall, P. A., Strack, O. D. L.: *Discrete numerical model for granular assemblies.* Geotechnique, vol. 29, no. 1, pp. 47–65, 1979.

[2] Coetzee, C. J.: *Calibration of the discrete element method and the effect of particle shape*. Powder Technol., vol. 297, pp. 50-70, 2016.

[3] Tamás, K., Földesi, B., Rádics, J. P., Jóri, I. J., Fenyvesi, L.: *A Simulation Model for Determining the Mechanical Properties of Rapeseed using the Discrete Element Method.* Period. Polytech. Civ. Eng., vol. 59, no. 4, pp. 575–582, 2015.

[4] Horabik, J., Molenda, M.: *Parameters and contact models for DEM simulations of agricultural granular materials: A review*. Biosyst. Eng., vol. 147, no. Supplement C, pp. 206–225, 2016.

[5] Bourrier, F., Kneib, F., Chareyre, B., Fourcaud, T.: *Discrete modeling of granular soils reinforcement by plant roots*. Ecol. Eng., vol. 61, no. Part C, pp. 646–657, 2013.

[6] Szabó, V.: *Fluidizációs szárítás hő- és anyagátadási folyamatainak modellezése (Modeling of heat and mass transfer in fluidized bed dryers)*. PhD dissertation, Budapest University of Technology and Economics, Budapest, Hungary, 2019.

[7] Suhr, B., Six, K.: *On the effect of stress dependent interparticle friction in direct shear tests*. Powder Technol., vol. 294, no. Supplement C, pp. 211–220, 2016.

[8] Yang, H., Xu, W.-J., Sun, Q.-C., Feng, Y.: *Study on the meso-structure development in direct shear tests of a granular material*. Powder Technol., vol. 314, no. Supplement C, pp. 129–139, 2017.

[9] Saadat, M., Taheri, A.: *A cohesive discrete element based approach to characterizing the shear behavior of cohesive soil and clay-infilled rock joints.* Comput. Geotech., vol. 114, p. 103-109, 2019.

[10] Šmilauer, V. *et al.*: *Dem formulation. In Yade Documentation 2nd ed.* Yade Proj., p. 37, 2015.

[11] Šmilauer, V., Gladky, A., Kozicki, J., Modenese, C., Stránský, J.: *Using and programming. In Yade Documentation 2nd ed.* Yade Proj., p. 149, 2015.

[12] Jiang, M., Shen, Z., Wang, J.: *A novel three-dimensional contact model for granulates incorporating rolling and twisting resistances*. Comput. Geotech., vol. 65, pp. 147–163, 2015.

[13] Chareyre, B., Villard, P.: *Dynamic Spar Elements and Discrete Element Methods in Two Dimensions for the Modeling of Soil-Inclusion Problems.* J. Eng. Mech., vol. 131, no. 7, pp. 689–698, 2005.